Evanescent waves and deaf bands in sonic crystals

V. Romero-García, L. M. Garcia-Raffi, and J. V. Sánchez-Pérez

Citation: AIP Advances **1**, 041601 (2011); doi: 10.1063/1.3675801
View online: http://dx.doi.org/10.1063/1.3675801
View Table of Contents: http://aipadvances.aip.org/resource/1/AAIDBI/v1/i4
Published by the American Institute of Physics.

Evanescent waves and deaf bands in sonic crystals

V. Romero-García,[1,a] L. M. Garcia-Raffi,[2] and J. V. Sánchez-Pérez[3]
[1]*Instituto de Investigación para la Gestión Integrada de zonas Costeras, Universidad Politécnica de Valencia, Paranimf 1, 46730, Gandia, Spain*
[2]*Instituto Universitario de Matemática Pura y Aplicada, Universidad Politécnica de Valencia, Camino de Vera s/n, 46022, Valencia, Spain*
[3]*Centro de Tecnologías Físicas: Acústica, Materiales y Astrofísica, Universidad Politécnica de Valencia, Camino de Vera s/n, 46022, Valencia, Spain*

(Received 18 October 2011; accepted 4 December 2011; published online 23 December 2011)

The properties of sonic crystals (SC) are theoretically investigated in this work by solving the inverse problem $k(\omega)$ using the extended plane wave expansion (EPWE). The solution of the resulting eigenvalue problem gives the complex band structure which takes into account both the propagating and the evanescent modes. In this work we show the complete mathematical formulation of the EPWE for SC and the supercell approximation for its use in both a complete SC and a SC with defects. As an example we show a novel interpretation of the deaf bands in a complete SC in good agreement with multiple scattering simulations. *Copyright 2011 Author(s). This article is distributed under a Creative Commons Attribution 3.0 Unported License*. [doi:10.1063/1.3675801]

I. INTRODUCTION

Exploitation of wave propagation properties of periodic materials has showed in the last decades an increasing number of application in condensed matter physics, specially in photonics[1,2] and phononics.[3–5] The particular dispersion relation of these systems, known as the band structure, reveals several properties depending on the frequency. In the range of wavelength much lower than the distance between the scatterers (subwavelength regime), the heterogeneous periodic material can be considered as an effective medium with effective parameters.[6] When resonant scatterers are used to construct the periodic material, the effective medium in the subwavelength regime constitutes the implementation of the Veselago's theoretical prediction of a material with negative properties.[7] Potential application of such a systems are the left handed materials[8] and subwavelength imaging.[9–11] For the case of wavelength comparable with the distance between scatterers, there are ranges of frequencies where only evanescent modes can be excited in the system.[3,22] These ranges of frequencies are known as band gaps (BG) by analogy with semiconductors in solid state physics. Finally making use of the dispersion curves one can design periodic media presenting negative refraction[12,13] or self-collimation[14,15] of waves.

Traditionally the band structure has been calculated using the $\omega(\vec{k})$ methods with, for example, the plane wave expansion (PWE) procedure.[16] In this case, the resulting eigenvalue problem provides only real eigenvalues[17] and, as a consequence, only the propagating properties of the system can be analyzed. Recent works[18,19] develop an extended plane wave expansion (EPWE) method to solve the inverse problem $k(\omega)$ taking into account both the propagating and the evanescent properties of the system. This method provides a more complete picture of the physical properties of the system than the classical $\omega(\vec{k})$ procedures as well as novel interpretation of the existing phenomena. Experimental results are in very good agreement with the prediction of EPWE for the case of both complete[18] and defective[20,21] sonic crystals (SC), which are the periodic system for acoustic waves.

[a]Electronic mail: virogar1@mat.upv.es; http://personales.upv.es/virogar1

In this work we show an example in which the complex band structure predicted by using the EPWE introduces a new interpretation of the physical properties of periodic structures due to consider both propagating and evanescent properties. We focus the attention on the deaf bands.[22] Traditionally, deaf bands are acoustic branches of modes in the band structure that cannot be excited depending on the symmetry of the mode with respect to the source, hence they do not transport acoustic energy through the crystal. In the usual case that a plane wave is normally incident on the phononic crystal, a mode that is antisymmetric with respect to the propagation direction will be deaf.[23] The analogous effect has been also observed in photonic materials.[24,25] In this work we show that deaf bands are ranges of frequencies in which the evanescent modes with the correct symmetry are excited, being the attenuation related to the imaginary part of the Bloch vector. We compare the EPWE predictions with those predicted using the multiple scattering theory (MST),[26–28] obtaining good agreement between these two independent methodologies. We find the evanescent modes of fundamental interest to characterize the properties of periodic structures. In fact the relevance of the evanescent modes in periodic system has been recently shown in potential applications in subwavelength imaging.[9–11]

The work is organized as follows. First of all we show the complete formulation of the EPWE method for the case of SC. For simplicity we focus the attention on the SC, however the methodology can be applied to other periodic system having several polarizations. The application of the supercell approximation in the EPWE is also presented, showing then the possibility to use the EPWE in SC with defects. Once the EPWE is presented, we analyze the case of the deaf bands using the EPWE and comparing the new interpretation with the classical ones. Finally, the conclusions are shown.

II. THEORETICAL MODEL: EXTENDED PLANE WAVE EXPANSION

A. Eigenvalue problem for complete sonic crystals

Propagation of sound is described by the equation

$$\frac{1}{\rho c^2}\frac{\partial^2 p}{\partial t^2} = \nabla\left(\frac{1}{\rho}\nabla p\right) \tag{1}$$

where c is the sound velocity, ρ is the density of the medium and p is the pressure.

In this work we are interested in the propagation of sound waves in a system composed of a periodic array of straight, infinite cylinders made of an isotropic solid A, embedded in an acoustic isotropic fluid background B. There is translational invariance in the direction z parallel to the axis of the cylinders and the system has 2D periodicity in the transverse plane. By using this periodicity, it is possible to expand the properties of the medium in Fourier series,

$$\sigma = \frac{1}{\rho(\vec{r})} = \sum_{\vec{G}} \sigma_{\vec{k}}(\vec{G}) e^{\imath \vec{G}\vec{r}}, \tag{2}$$

$$\eta = \frac{1}{B(\vec{r})} = \sum_{\vec{G}} \eta_{\vec{k}}(\vec{G}) e^{\imath \vec{G}\vec{r}}, \tag{3}$$

where $\vec{G}$ is the 2D reciprocal-lattice vector and $B(\vec{r}) = \rho(\vec{r})c(\vec{r})^2$ is the bulk modulus. The pressure p can be obtained by applying the Bloch theorem and harmonic temporal dependence,

$$p(\vec{r}, t) = e^{\imath(\vec{k}\vec{r}-\omega t)} \sum_{\vec{G}} p_k(\vec{G}) e^{\imath \vec{G}\vec{r}}. \tag{4}$$

It is easy to show that[16]

$$\alpha(\overrightarrow{G}) = \begin{cases} \beta_A ff + \beta_B(1-ff) & \text{if } \overrightarrow{G} = \overrightarrow{0} \\ (\beta_A - \beta_B) F(\overrightarrow{G}) & \text{if } \overrightarrow{G} \neq \overrightarrow{0} \end{cases} \tag{5}$$

where $\beta_i = (\sigma, \eta)$ (i indicating the material), $F(\overrightarrow{G})$ is the structure factor and ff is the filling fraction defined as ratio between the volume occupied by the scatterer in the unit cell and the volume of the

unit cell. For circular cross section of radius r, the structure factor is

$$F(\vec{G}) = \frac{1}{A_{uc}} \int_{A_{cyl}} e^{-\imath \vec{G}\,\vec{r}}\, d\vec{r} = \frac{2ff}{Gr} J_1(Gr). \tag{6}$$

A_{uc} is the area of the unit cell, A_{cyl} is the area of the considered cylinder and J_1 is the Bessel function of the first kind of order 1.

Using Equations (1)–(4) we obtain[16]

$$\sum_{\vec{G}'} \left((\vec{k}+\vec{G})\sigma_k(\vec{G}-\vec{G}')(\vec{k}+\vec{G}') - \omega^2 \eta_{\vec{k}}(\vec{G}-\vec{G}') \right) p_{\vec{k}}(\vec{G}') = 0. \tag{7}$$

For $\vec{G}$ taking all the possible values, Equation (7) constitutes a set of linear, homogeneous equations for the eigenvectors $p_{\vec{k}(\vec{G})}$ and the eigenfrequencies $\omega(\vec{k})$. The solution of this eigenvalue problem constitutes the classical band structure obtained from the $\omega(\vec{k})$ method.

B. Inverse problem for complete structures

Equation (7) can be expressed by the following matrix formulation

$$\sum_{i=1}^{3} \Gamma_i \Sigma \Gamma_i P = \omega^2 \Omega P, \tag{8}$$

where i=1,2,3. The matrices Γ_i, Σ and Ω are defined as

$$(\Gamma_i)_{mn} = \delta_{mn}(k_i + G_i^m). \tag{9}$$

The explicit matrix formulation is shown as follow:

$$\Gamma_i = \begin{pmatrix} k_i + G_i & 0 & \dots & 0 \\ 0 & k_i + G_i & \dots & 0 \\ \vdots & \vdots & \ddots & \vdots \\ 0 & \dots & \dots & k_i + G_i \end{pmatrix}, \tag{10}$$

$$\Sigma = \begin{pmatrix} \sigma(\vec{G}_1 - \vec{G}_1) & \dots & \sigma(\vec{G}_1 - \vec{G}_{N\times N}) \\ \vdots & \ddots & \vdots \\ \sigma(\vec{G}_{N\times N} - \vec{G}_1) & \dots & \sigma(\vec{G}_{N\times N} - \vec{G}_{N\times N}) \end{pmatrix}, \tag{11}$$

$$\Omega = \begin{pmatrix} \eta(\vec{G}_1 - \vec{G}_1) & \dots & \eta(\vec{G}_1 - \vec{G}_{N\times N}) \\ \vdots & \ddots & \vdots \\ \eta(\vec{G}_{N\times N} - \vec{G}_1) & \dots & \eta(\vec{G}_{N\times N} - \vec{G}_{N\times N}) \end{pmatrix}, \tag{12}$$

$$P = \begin{pmatrix} P(\vec{G}_1) \\ \vdots \\ P(\vec{G}_{N\times N}) \end{pmatrix}. \tag{13}$$

In this Section we invert the classical $\omega(\vec{k})$ problem to the $k(\omega)$ method. From Equation (8) we define the following vector,

$$\Phi_i = \Sigma \Gamma_i P. \tag{14}$$

With this definition it is possible to reformulate the eigenvalue problem (8) as the equation system

$$\Phi_i = \Sigma \Gamma_i P$$

$$\omega^2 \Omega P = \sum_{i=1}^{3} \Gamma_i \Phi_i. \tag{15}$$

In order to obtain an eigenvalue problem for $k(\omega)$, we write $\vec{k} = k\vec{\alpha}$, where $\vec{\alpha}$ is a unit vector which indicates the incidence direction. Then Eq. (10) can be written as

$$\Gamma_i = \Gamma_i^0 + k\alpha_i I, \tag{16}$$

where I is the identity matrix, and

$$\Gamma_i^0 = \begin{pmatrix} G_i & 0 & \dots & 0 \\ 0 & G_i & \dots & 0 \\ \vdots & \vdots & \ddots & \vdots \\ 0 & \dots & \dots & G_i \end{pmatrix}, \tag{17}$$

$$\alpha_i = \begin{pmatrix} \alpha_i & 0 & \dots & 0 \\ 0 & \alpha_i & \dots & 0 \\ \vdots & \vdots & \ddots & \vdots \\ 0 & \dots & \dots & \alpha_i \end{pmatrix}. \tag{18}$$

Equation (8) can be written as

$$\begin{pmatrix} \omega^2\Omega - \sum_{i=1}^{3} \Gamma_i^0 \Sigma \Gamma_i^0 & 0 \\ -\sum_{i=1}^{3} \Sigma \Gamma_i^0 & I \end{pmatrix} \begin{pmatrix} P \\ \Phi' \end{pmatrix} = k \begin{pmatrix} \sum_{i=1}^{3} \Gamma_i^0 \Sigma \alpha_i & I \\ \sum_{i=1}^{3} \Sigma \alpha_i & 0 \end{pmatrix} \begin{pmatrix} P \\ \Phi' \end{pmatrix} \tag{19}$$

where $\Phi' = \sum_{i=1}^{3} \alpha_i \Phi_i$.

Equation (19) represents a generalized eigenvalue problem with $2N$ eigenvalues k, possibly complex numbers, for each frequency. Complex band structures on the incidence direction $\vec{\alpha}$ can be obtained by solving the eigenvalue equation for a discrete number of frequencies and then sorting them by continuity of k. In contrast with the $\omega(\vec{k})$ method, in this formulation $k(\omega)$ is not forced to follow the first Brillouin zone.

To analyse the propagation of waves inside periodic structures with defects, authors have traditionally used PWE with supercell approximation. The supercell method requires an interaction as low as possible between defects. This results in a periodic arrangement of supercells which contains the point defect. With this method it is possible to obtain the relation $\omega(\vec{k})$ for crystals with local defects and for instance one can explain the physics of wave guides[29,30] or filters.[31]

In this Section, we apply the approximation of supercell to the EPWE. As in the classical methods, this methodology allows us to obtain the relation $k(\omega)$ for systems with defects. The study of the imaginary part of the wave vector in the complex band structure allows us to characterize the evanescent behaviour of both the complete SC and SC with defects.

C. Supercell approximation

We consider a SC with primitive lattice vectors $\vec{a}_i$ $(i = 1, 2, 3)$. The supercell is a cluster of $n_1 \times n_2 \times n_3$ scatterers periodically placed in the space. Then, the primitive lattice vectors in the supercell approximation are $\vec{a'}_i = n_i \vec{a}_i$, and the complete set of lattices in the supercell approximation is $\{R' | R' = l_i \vec{a'}_i\}$, where n_i and l_i are integers. The primitive reciprocal vectors are then

$$\vec{b'}_i = 2\pi \frac{\varepsilon_{ijk} \vec{a'}_j \times \vec{a'}_k}{\vec{a'}_1 \cdot (\vec{a'}_2 \times \vec{a'}_3)} \tag{20}$$

where ε_{ijk} is the three-dimensional Levi-Civita completely anti-symmetric symbol. The complete set of reciprocal lattice vectors in the supercell is $\{\vec{G} | \vec{G}_i = N_i \vec{b'}_i\}$ where N_i are integers. Without loss of generality, the next formulation is constrained to 2D systems.

1. Complete arrays

With the previous definition of supercell, the expression similar to Equation (5) for the case of the supercell approximation is obtained. The filling fraction of a cylinder in a supercell is $ff = \pi r^2/A$, where A is the area occupied by the supercell. If we consider a supercell with N cylinders organized in an array of size $n_1 \times n_2$ then

$$\beta(\vec{G}) = \begin{cases} \beta_A N\ ff + \beta_B(1 - N\ ff) & \text{if } \vec{G} = \vec{0} \\ (\beta_A - \beta_B)\, F(\vec{G}) & \text{if } \vec{G} \neq \vec{0} \end{cases} \tag{21}$$

where $F(\vec{G})$ is the structure factor of the supercell.

In this approximation, the structure factor of the supercell has to be computed taking into account its size. If we consider a 2D SC with cylindrical scatterers with radius r and size of the supercell $n_1 \times n_2$, being n_i an odd number, the structure factor is expressed by

$$F(\vec{G}) = \sum_{i=-(n_1-1)/2}^{(n_1-1)/2} \sum_{j=-(n_2-1)/2}^{(n_2-1)/2} e^{\imath(ia|\vec{G}_1|+ja|\vec{G}_2|)} P(\vec{G}) \tag{22}$$

where

$$P(\vec{G}) = \frac{2\ ff}{Gr} J_1(Gr). \tag{23}$$

where a is the lattice constant inside the supercell and $G = |\vec{G}|$.

2. Arrays with defects

If the supercell presents N_p point defects at the sites labelled by (l_s, m_s) in the periodic system, with $s = 1, ..., N_p$, then the Fourier coefficients of the expansion of the physical parameters involved in the problem satisfy the following equation

$$\beta(\vec{G}) = \begin{cases} \beta_A(N - N_p)ff + \beta_B(1 - (N - N_p)ff) & \text{if } \vec{G} = \vec{0} \\ (\beta_A - \beta_B)\, F(\vec{G}) & \text{if } \vec{G} \neq \vec{0} \end{cases} \tag{24}$$

The structure factor of such a supercell with N_p point defects is

$$F(\vec{G}) = \left(\sum_{i=-(n_1-1)/2}^{(n_1-1)/2} \sum_{j=-(n_2-1)/2}^{(n_2-1)/2} e^{\imath(ia|\vec{G}_1|+ja|\vec{G}_2|)} - \sum_{s=1}^{N_p} e^{\imath(l_s a|\vec{G}_1|+m_s a|\vec{G}_2|)} \right) P(\vec{G}). \tag{25}$$

The interaction among the defect points in the supercell approximation must be as low as possible between the neighboring supercells in order to prevent the overlap in between, thus the size of the supercell should be big enough to place the point defects separated in consecutive supercells.

By introducing the previous expressions in the matrix formulation of either the PWE (8) or the EPWE (19), the band structure of a periodic structure with and without a point defect using the supercell approximation can be calculated.

III. RESULTS

Consider a 2D periodic distribution of rigid cylindrical scatterers embedded in air forming a square array with lattice constant a. The filling fraction, defined as the ratio between the volume occupied by the scatterer and the volume of the unit cell is, $ff = \pi r^2/a^2 \simeq 60\%$. In this work we use reduced magnitudes to show the results, i.e. $\Psi = \nu a/c$ is the reduced frequency and $K = ka/2\pi$ is the reduced Bloch vector, being $\nu = \omega/2\pi$ the frequency of the wave and c the speed of sound. This system presents two main direction of symmetry: 0° of incidence (ΓX direction) and 45° of incidence (ΓM direction). The band structure of such a system has been extensively analyzed in the literature,[22] therefore let us to fix our attention only in the ΓM direction.

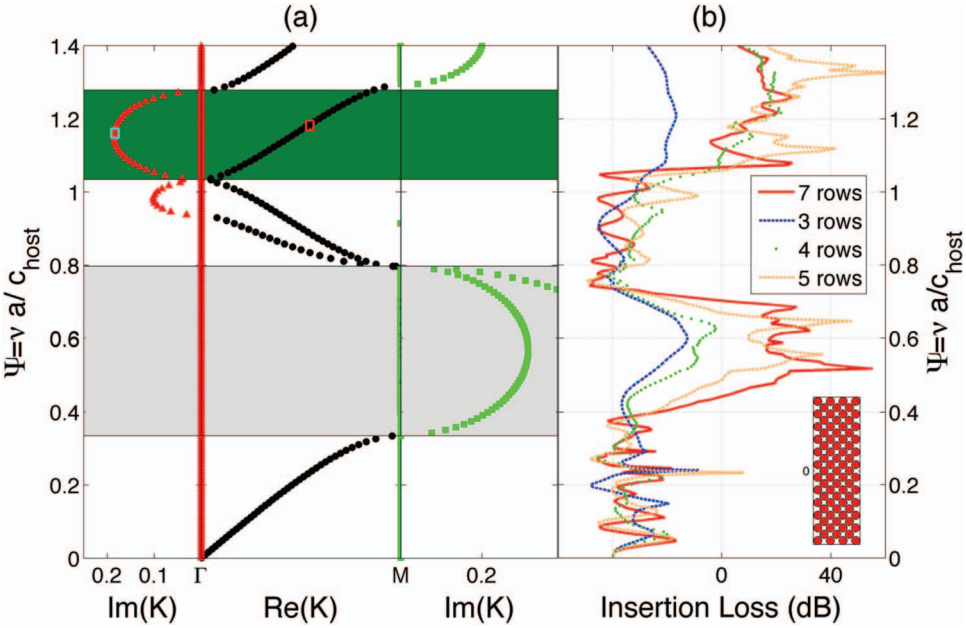

FIG. 1. Analysis of deaf bands using the complex band structure calculated using the EPWE. (a) Complex band structure for a SC with square periodicity which filling fraction is $ff = \pi r^2/a \simeq 60\%$, being a the lattice constant. Grey area represents the BG. Green area represents the attenuation range produced by the presence of a deaf band. (b) Red continuous line represents the *IL* evaluated using the structure shown in the inset at point $(a, 0)$. Other coloured lines shows the *IL* for several structures with less number of rows at the ΓM direction of incidence.

A. Complex band structure

The complex band structure of this system in the ΓM direction, calculated using EPWE, is illustrated in Figure 1(a). The band structure has been represented using the following code: (*i*) The classical band structure correspond to modes characterized by values of $Re(K)$ in the Brillouin zone and $Im(K) = 0$ (i.e. purely real modes). Modes with these properties are shown in this work with black filled circles. (*ii*) The modes characterized by $Im(K) \geq 0$ and $Re(K) = 0$ are shown with red filled triangles. These modes represent connections between propagating bands at the Γ point. (*iii*) The modes characterized by $Im(K) \geq 0$ and $Re(K) = 1/2$ (respectively, $Re(K) = 1/\sqrt{2}$) are shown with green filled squares. These modes represents connections between propagating bands at the X (respectively, M) point. In this work we show the relevance of the evanescent connections in the edges of the Brillouin zone with complex valuated Bloch vector.

The transmission properties of the system have been also evaluated theoretically using the Insertion Loss which is the difference between the sound level with and without the sample recorded at the same point. Then, in this work the IL can be evaluated as

$$IL(dB) = 20 \log \left(\frac{|p_0|}{|p|} \right) \tag{26}$$

where $|p_0|$ and $|p|$ are the pressure without and with the structure respectively. The structure is placed between the source and the receiver. The pressure field has been evaluated using the MST. Red continuous line in the Figure 1(b) represents the *IL* evaluated behind the structure at point $(a, 0)$ for the structure represented in the inset. Other coloured lines represent the *IL* for smaller structures with less number of rows.

It is worth noting that for this case the real part of the complex band structure is the same as the classical bands predicted using the $\omega(\vec{k})$ method (using for example PWE). The grey area in Figure 1(a) represents the BG of the structure. Notice that in this range of frequencies the complex band structure predicts bands with complex values of k, i.e. evanescent modes never observed in classical methodologies. We emphasize the fact that the number of the overall bands for each

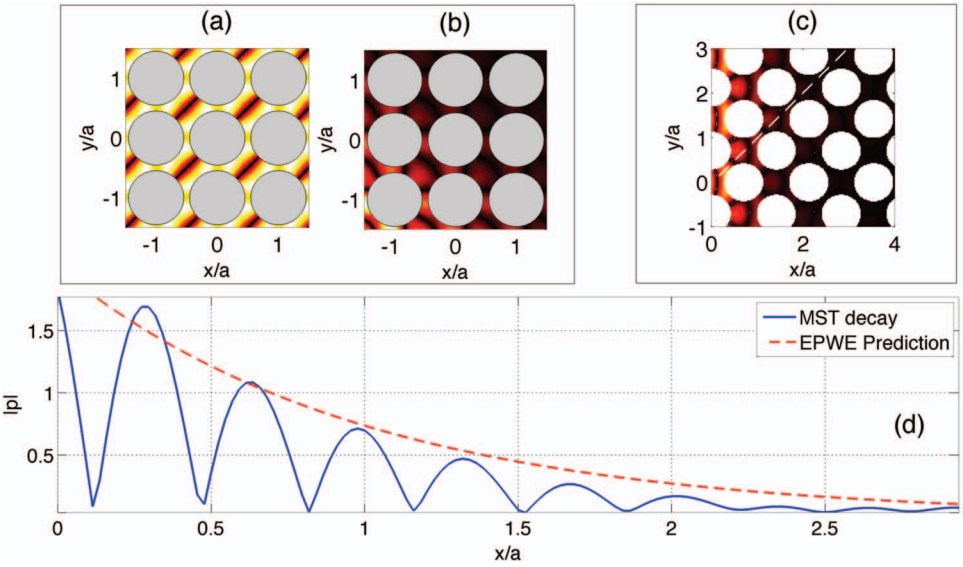

FIG. 2. (a) Acoustic field calculated with the EPWE, corresponding to the mode in the deaf band marked in Figure 1(a) with a red square ($\Psi = 1.14$, $Re(K) = 0.39$). (b) Acoustic field calculated with the EPWE, corresponding to the mode in the deaf band marked in Figure 1(a) with a blue square ($\Psi = 1.14$, $Im(K) = 0.19$). (c) Acoustic field predicted using the MST at frequency $\Psi = 1.14$. (d) Blue continuous line represent the values of $|p|$ inside the periodic structure along the white dashed line in (c). Red dashed line represents the exponential decay predicted using the EWPE.

frequency is preserved and this fact allows us to define the BG as ranges of frequencies where only evanescent modes are excited.

On the other hand the *IL* predicted using the MST (Figure 1(b)) shows the attenuation peaks in ranges of frequencies in the BG, in agreement with the band structure predictions. The analysis of the evanescent modes in the BG has recently shown very good agreement with experimental results,[9–11] demonstrating the important role of the evanescent connections to interpret the propagation properties of the periodic structures.

Regarding the attenuation peak shown in the ΓM direction around $\Psi = 1.2$ (green shadowed area in the band structure 1(a)), the classical band structure (black dotted lines) predicts the existence of a propagating band at these frequencies. That band would produce the transmission of waves, however this apparently strange behavior has been classically explained by the particular symmetry of the modes that can be excited in the SC at this frequency. In this work we show that the attenuation is not only due to symmetry reasons but also to the evanescent waves in relation with the imaginary part of the complex band structure. The evanescent mode with the excitable symmetry is the only state that contributes to the attenuation. Thus, the complex band structures are necessary to completely characterize the system.

B. Deaf bands

Generally speaking, in eigenvalue problems each eigenvalue has an associated eigenvector. In the case of the EPWE, the Fourier transform of the eigenvector (Equation (4)) can be used to obtain the pressure field pattern of each eigenmode. Figure 2(a) shows the acoustic field for the mode with completely real Bloch vector (classical mode) marked with a red square in Figure 1(a) ($\Psi = 1.14$, $Re(K) = 0.39$). Notice that the incidence of the wave is along the ΓM direction (i.e. with direction $\vec{u} = \frac{1}{\sqrt{(2)}}(1, 1)$). Then, the pressure field pattern of this mode has the planes of equal phase along the perpendicular direction and consequently cannot be excited by such a wave and this branch of the band structure will be deaf. The modes in this branch has the same symmetry of the field, thus the green area in Figure 1(a) shows the ranges of frequencies attenuated by the presence of the deaf band.

Following the interpretation of the classical methods, no modes could be excited in this range of frequencies. However, if one analyzes the *IL* for this range of frequencies, some transmission is observed with a dependence on the number of rows that form the structure. On the other hand, the complex band structure shows an evanescent connection at the Γ edge of the Brillouin zone (see red triangles in Figure 1(a)) showing that evanescent modes can be excited at this range of frequencies. Analogously to the analysis of the pressure field pattern in the classical methods, one can do the same considering the complex value of the Bloch vector predicted using the EPWE in the evanescent connection at $\Psi = 1.14$ with $Im(K) = 0.19$. The pressure field pattern for this case is shown in Figure 2(b). For this case, one can observe that the symmetry of the field is in agreement with the symmetry of the incident wave and that the field decays as it penetrates in the periodic system along the incidence direction. Then the EPWE shows that the called deaf bands are ranges of frequencies where evanescent waves with the correct symmetry are excited in the system.

To check the results of the EPWE we have calculated the acoustic field inside a finite structure using the MST. Figure 2(c) represents a zoom of the acoustic field inside the structure shown in the inset of Figure 1(b). One can observe the good correspondence of the pressure field pattern predicted by MST and the one calculated from the Fourier transform of the eigenvector of the evanescent mode predicted by EPWE. Then, the decay along the ΓM direction is characterized by means of the $Im(K) = 0.19$. However, we only can evaluate continuously the decay along the ΓX as it is marked with the white dashed line in Figure 2(c). Notice that due to the symmetry of the unit cell, the decay along the ΓX direction when the incidence is along the ΓM direction is characterized by $\frac{1}{\sqrt{2}}\, Im(K)$.

Figure 2(d) shows the decay of the acoustic field along the ΓX direction (white dashed line) when the wave is impinging the structure along the ΓM direction. Blue continuous line represents the values of $|p|$ predicted by MST. Notice the damping of the acoustic field as the waves penetrates in the structure. Using the decay predicted by the EWPE along this direction ($\frac{1}{\sqrt{2}}\, Im(K)$) one can plot an exponential decay, $be^{-\frac{1}{\sqrt{2}}\, Im(K)\, x}$ where $b = 2$ Pa is a fitting parameter. Red dashed line represents the decay predicted by the EPWE. One can observe that the decay of the EPWE is very similar to the decay of the acoustic field inside the structure evaluated using MST.

Then, at frequencies corresponding to the deaf band, the mode supported by the structure corresponds to the evanescent mode predicted by EPWE with the proper symmetry to be excited by the incident wave. Thus, we can conclude that within deaf band frequency ranges, the classical band structure cannot explain the exponentially decreasing transmission that is observed in experiments and calculations for finite SC. The correct interpretation appears in terms of evanescent modes: There are ranges of frequencies in which the propagating bands are antisymmetric but at least some of the evanescent modes are symmetric with respect to the incident wave. These modes can be excited and they are responsible of the observed attenuation.

IV. CONCLUSIONS

The propagation of waves inside periodic structures consists of both propagating and evanescent modes. The complex band structure obtained using the EPWE takes into account these waves and shows additional bands never predicted by the classical methods $\omega(\vec{k})$. In this work we have shown the complete formulation of the extension of the $\omega(\vec{k})$ to the $k(\omega)$ method for the case of both complete 2D SC and SC with defects. The latter makes use of the supercell approach. Due to the conservation of the overall number of bands for a determined frequency, a novel interpretation of deaf bands arises from the analysis of the complex band structures: ranges of frequencies where evanescent waves with the correct symmetry are excited in the system. The MST predictions of the behaviour of the acoustic field are in very good agreement with the EPWE predictions. The results presented in this work show the relevance of the evanescent waves to interpret the physical properties of periodic system, being this short-range waves of fundamental interest for the correct understanding of systems based on periodicity.

ACKNOWLEDGMENTS

This work was supported by MCI-Secretaría de Estado de Investigación (Spanish government) and the FEDER funds, under grant MAT2009-09438. LMGR would like to thank the UPV for the grant PAID-00-11. VRG is grateful for the support of "Programa de Contratos Post-Doctorales con Movilidad UPV (CEI-01-11)."

[1] E. Yablonovitch, J. Phys. Condens. Matter **5**, 2443 (1993).
[2] J. D. Joannopoulos, S. G. Johnson, J. N. Winn, and R. D. Meade, *Photonic Crystals. Molding the Flow of Light* (Princeton University press, 2008).
[3] R. Martínez-Sala, J. Sancho, J. V. Sánchez, V. Gómez, J. Llinares, and F. Meseguer, Nature **378**, 241 (1995).
[4] M. Sigalas, M. S. Kushwaha, E. N. Economou, M. Kafesaki, I. E. Psarobas, and W. Steurer, Z. Kristallogr. **220**, 765 (2005).
[5] Y. Pennec, J. Vasseur, B. Djafari-Rouhani, L. Drobrzyski, and P. Demier, Surface Science Reports **65**, 229 (2010).
[6] D. Torrent, A. Hakansson, F. Cervera, and J. Sánchez-Dehesa, Phys. Rev. Lett. **96**, 204302 (2006).
[7] V. Veselago, Sov. Phys. Usp. **10**, 509 (1968).
[8] C. M. Soukoulis, M. Kafesaki, and E. N. Economou, Adv. Mater. **18**, 1941 (2006).
[9] A. Sukhovich, B. Merheb, K. Muralidharan, J. Vasseur, Y. Pennec, P. Demier, and J. Page, Phys. Rev. Lett. **102**, 154301 (2009).
[10] J. F. Robillard, J. Bucay, P. Demier, A. Shelke, K. Muralidharan, B. Merheb, J. Vasseur, A. Suckovich, and J. Page, Phys. Rev. B **83**, 224301 (2011).
[11] J. Zhu, J. Christensen, J. Jung, L. Martin-Moreno, X. Lin, L. Fok, X. Zhang, and F. J. García-Vidal, Nature Physics **7**, 52 (2011).
[12] S. Yang, J. H. Page, Z. Liu, M. L. Cowan, C. Chan, , and P. Sheng, Phys. Rev. Lett. **93**, 024301 (2004).
[13] L. Feng, X. Liu, Y. Chen, Z. Huang, Y. Mao, Y. Chen, J. Zi, and Y. Zhu, Phys. Rev. B **72**, 033108 (2005).
[14] I. Pérez-Arjona, V. J. Sánchez-Morcillo, J. Redondo, V. Espinosa, and K. Staliunas, Phys. Rev. B **75**, 014304 (2007).
[15] V. Espinosa, V. J. Sánchez-Morcillo, K. Staliunas, I. Pérez-Arjona, and J. Redondo, Phys. Rev. B **76**, 140302(R) (2007).
[16] M. Kushwaha, P. Halevi, G. Martínez, L. Dobrzynski, and B. Djafari-Rouhani, Phys. Rev. B **49** (4), 2313 (1994).
[17] H. Hernández-Cocoletzi, A. Krokhin, and P. Halevi, Phys. Rev. B **23**, 17181 (1995).
[18] V. Romero-García, J. Sánchez-Pérez, and L. Garcia-Raffi, J. Appl. Phys. **108**, 044907 (2010).
[19] V. Laude, Y. Achaoui, S. Benchabane, and A. Khelif, Phys. Rev. B **80**, 092301 (2009).
[20] V. Romero-García, J. Sánchez-Pérez, S. Castiñeira Ibáñez, and L. Garcia-Raffi, Appl. Phys. Lett. **96**, 124102 (2010).
[21] V. Romero-García, J. Sánchez-Pérez, and L. Garcia-Raffi, New J. Phys. **12**, 083024 (2010).
[22] J. V. Sánchez-Pérez, D. Caballero, R. Martínez-Sala, C. Rubio, J. Sánchez-Dehesa, F. Meseguer, J. Llinares, and F. Gálvez, Phys. Rev. Lett. **80**, 5325 (1998).
[23] F. Hsiao, A. Khelif, H. Moubchir, A. Choujaa, C. Chen, and V. Laude, J. Appl. Phys. **101**, 044903 (2007).
[24] W. Robertson, G. Arjavalingam, R. Meade, K. Brommer, A. Rappe, and J. Joannopoulos, Phys. Rev. Lett **68**, 2023 (1992).
[25] T. F. Krauss, R. de la Rue, and S. Brand, Nature **383**, 699 (1996).
[26] C. Linton and P. McIver, *Handbook of Mathematical Techniques for wave/structure interactions* (CRC Press, 2001).
[27] Y.-Y. Chen and Z. Ye, Phys. Rev. E **64**, 036616 (2001).
[28] P. Martin, *Multiple Scattering. Interaction of Time-Harmonic Waves with N Obstacles* (Cambridge University Press, UK, 2006).
[29] A. Khelif, M. Wilm, V. Laude, S. Ballandras, and B. Djafari-Rouhani, Phys. Rev. E **69**, 067601 (2004).
[30] J. O. Vasseur, P. A. Deymier, B. Djafari-Rouhani, Y. Pennec, and A.-C. Hladky-Hennion, Phys. Rev.B **77**, 085415 (2008).
[31] A. Khelif, A. Choujaa, B. Djafari-Rouhani, M. Wilm, S. Ballandras, and V. Laude, Phys. Rev. B **68**, 214301 (2003).